

TOPICAL REVIEW • OPEN ACCESS

Known mechanisms that increase nuclear fusion rates in the solid state

To cite this article: Florian Metzler *et al* 2024 *New J. Phys.* **26** 101202

View the [article online](#) for updates and enhancements.

You may also like

- [Semiclassical theory of frequency combs generated by parametric modulation of optical microresonators](#)
M Sumetsky

- [The Josephson junction as a quantum engine](#)
Robert Alicki, Micha Horodecki, Alejandro Jenkins *et al.*

- [Non-analytic behaviour in large-deviations of the susceptible-infected-recovered model under the influence of lockdowns](#)
Leo Patrick Mulholland, Yannick Feld and Alexander K Hartmann

Supplementary Notes for this paper are here:

<http://lenr-canr.org/acrobat/MetzlerFsupplemena.pdf>

A paper with similar contents is here:

"Models for nuclear fusion in the solid state"

<https://arxiv.org/abs/2501.08338>

A copy is here:

<http://lenr-canr.org/acrobat/Hagelsteinmodelsforn.pdf>



TOPICAL REVIEW

Known mechanisms that increase nuclear fusion rates in the solid state

OPEN ACCESS

RECEIVED

13 April 2023

REVISED

8 October 2023

ACCEPTED FOR PUBLICATION



1 November 2023

PUBLISHED

25 October 2024

Original content from
this work may be used
under the terms of the
[Creative Commons
Attribution 4.0 licence](#).

Any further distribution
of this work must
maintain attribution to
the author(s) and the title
of the work, journal
citation and DOI.

Florian Metzler^{1,*} , Camden Hunt¹, Peter L Hagelstein¹ and Nicola Galvanetto^{1,2,*} ¹ Massachusetts Institute of Technology, Cambridge, MA 02139, United States of America² University of Zurich, Winterthurerstrasse 190, 8057 Zurich, Switzerland

* Authors to whom any correspondence should be addressed.

E-mail: fmetzler@mit.edu and galvanet@mit.edu**Keywords:** condensed matter, nuclear fusion, nuclear resonance, quantum dynamics, dicke enhancementSupplementary material for this article is available [online](#)

Abstract

We investigate known mechanisms for enhancing nuclear fusion rates at ambient temperatures and pressures in solid-state environments. In deuterium fusion, on which the paper is focused, an enhancement of >40 orders of magnitude would be needed to achieve observable fusion. We find that different mechanisms for fusion rate enhancement are known across the domains of atomic physics, nuclear physics, and quantum dynamics. Cascading multiple such mechanisms could lead to an overall enhancement of 40 orders of magnitude or more. We present a roadmap with examples of how hypothesis-driven research could be conducted in—and across—each domain to probe the plausibility of technologically-relevant fusion in the solid state.

1. Introduction

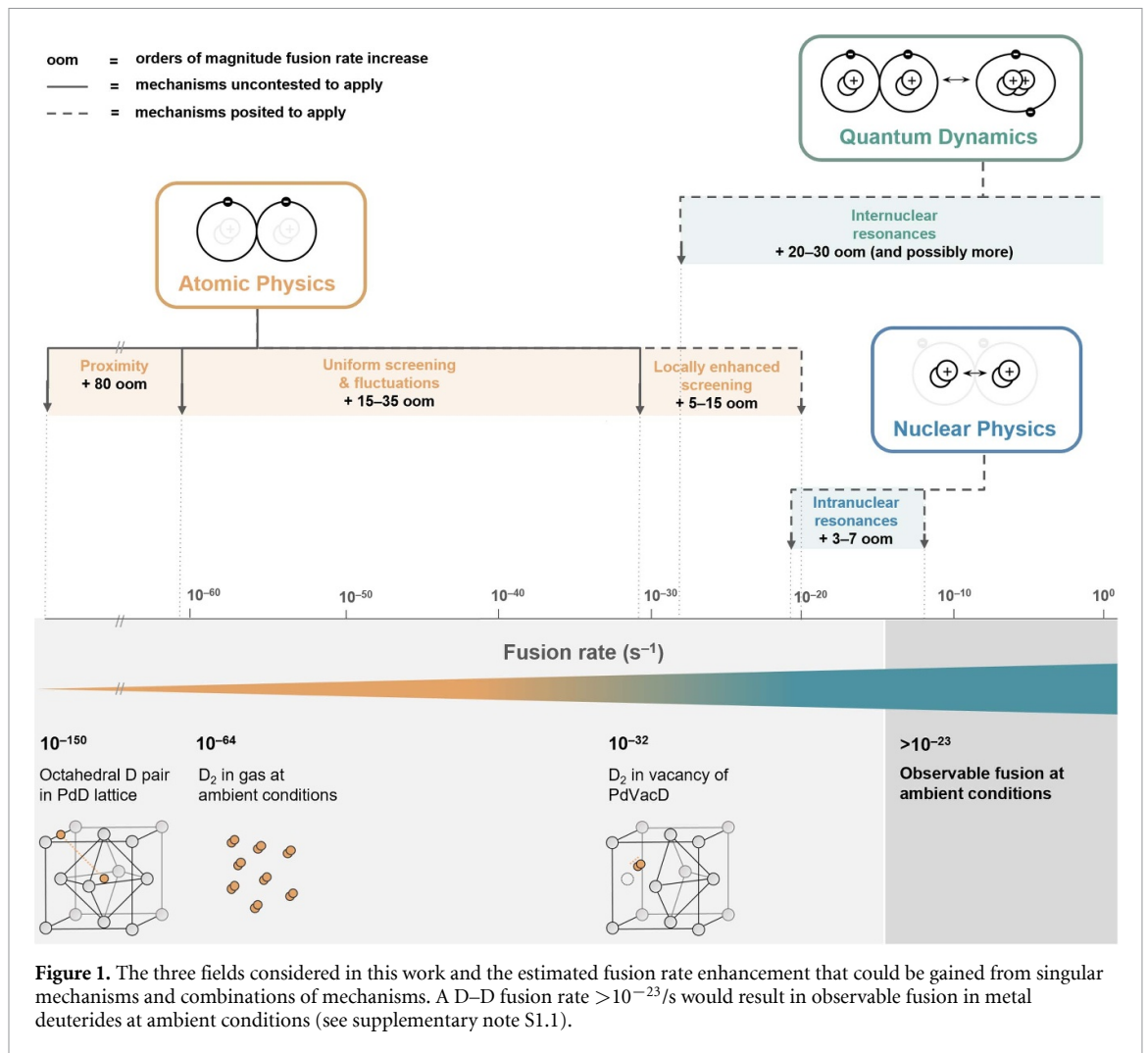
Nuclear fusion is purported to require extreme temperatures or pressures [1–5]. Claims that nuclear fusion is achievable at ambient temperatures and pressures in solid-state materials have surfaced repeatedly [6–10], but were in the past dismissed for lack of plausible explanations [11–13]. Among the strongest results are those reporting neutron and charged particle emissions from metal–hydrogen systems with low-energy stimulation [14–19]. Readily observable deuterium (D–D) fusion at ambient conditions would require a fusion rate increase of >40 orders of magnitude compared to the baseline spontaneous fusion rate of deuterium gas (estimated by Koonin & Nauenberg [20] as $\sim 10^{-64}$ /s per deuteron pair at the D_2 molecular distance of 74 pm^3). This paper examines D–D fusion in a solid-state environment through the perspectives of three disciplines—atomic physics, nuclear physics, and quantum dynamics—and asks the following question:

What known mechanisms can increase nuclear fusion rates in the solid state?

We offer no single mechanism that could increase fusion rates by 40 orders of magnitude from the very low base rate in deuterium gas. However, there are known mechanisms across fields that could individually increase fusion rates by as much as 30 orders of magnitude (figure 1). Identified mechanisms are discussed with supporting calculations.

The possibility of cascading two or more mechanisms provides a first-principles research map for studying solid-state fusion. We present combinations of enhancement mechanisms that could cumulatively provide a >40 orders of magnitude increase in fusion rates (figure 1). We conclude with examples of how hypothesis-driven research could be conducted in—and across—each field to probe the plausibility of technologically-relevant fusion in the solid state at ambient conditions.

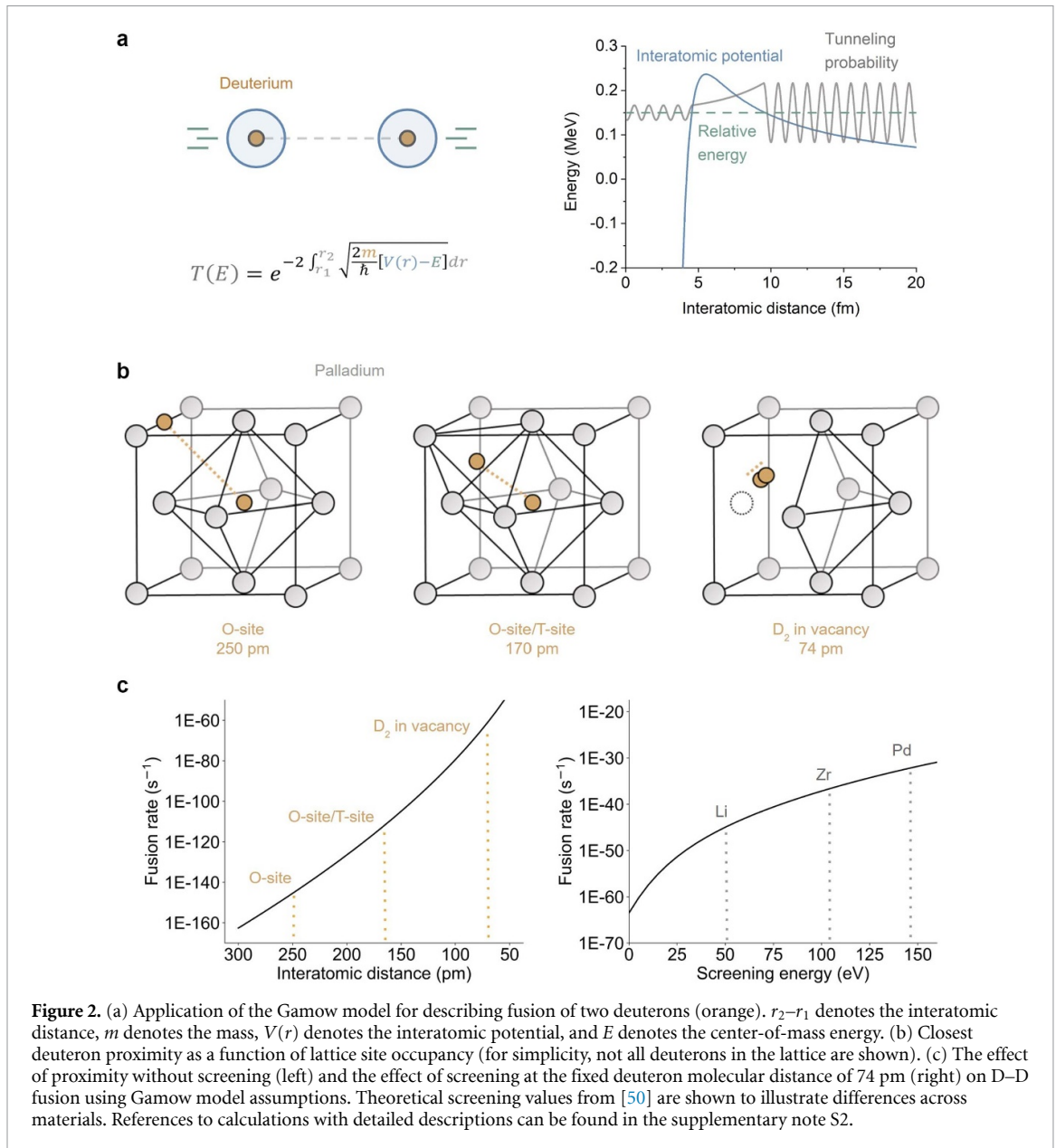
³ Consider that in a $\sim 3 \text{ g TiD}_2$ sample, for example, there are on the order of 10^{22} deuteron pairs. A fusion rate increase of 44 orders of magnitude to a rate of 10^{-20} /s would result in 100 fusion reactions per second, which is in the observable range—see supplementary note S1.1 for further details.



2. The atomic physics perspective

A simple description of nuclear fusion can be found in the Gamow model [21]. The Gamow model frames fusion as a quantum tunneling event through a potential barrier, with the barrier defined by the interatomic potential between two nuclei (figure 2(a)). Here, nuclei are considered point masses and point charges, and the fusion event is treated as near-instantaneous. Accordingly, the Gamow model is concerned with atomic physics (the interatomic potential) rather than nuclear physics (the fusion event). The interatomic potential can be simple—such as with nuclei in a diffuse plasma—or complex—such as with nuclei in a dense solid. In the latter case, the electronic structure of the solid will influence Gamow model variables.

The interatomic potential (figure 2(a)) [22–25] is defined by three partial potentials arising from electromagnetic and nuclear forces: (i) the electrostatic repulsion between nuclei due to positive charges of protons; (ii) the electrostatic attraction between such positive charges and negatively charged electrons as well as the electrostatic repulsion between such electrons; and (iii) the short-range ($<\sim 10$ fm) strong nuclear force attraction between all nucleons (see supplementary note S2.1 for more details). The resulting potential leads to an equilibrium position for pairs of nuclei at the range of interatomic bond lengths (~ 50 – 300 pm). If the interatomic distance of two nuclei is progressively decreased, the short-range attractive strong nuclear force will eventually dominate the electrostatic repulsion and the nuclei will fuse through quantum tunneling [26]. Quantum tunneling—a basic feature of all quantum systems—yields a probability distribution for overcoming the potential barrier as a function of the potential barrier and the interatomic distance (figure 2(a)). The product of the tunneling probability and the trial frequency (i.e., the number of tunneling attempts) is the fusion rate. The trial frequency results from collisions [27] (e.g., in a plasma) or oscillations [28] (e.g., in a solid). The two primary variables in the equation in figure 2(a) are the relative energy E between the two nuclei and the size and shape of the potential barrier $V(r)$ between the two nuclei. Most attempts at technologically-relevant fusion focus on maximizing E (e.g., through heating to $>100\,000\,000$ K) instead of manipulating $V(r)$ [1, 29].



Situations with more than two interacting atoms—such as deuterons within a palladium lattice—introduce new considerations to the Gamow model. $V(r)$ is now a function of all interacting nuclei and electrons [30]. Moreover, the interatomic distance ($r_2 - r_1$) is now dictated by where the deuterons reside in the lattice. When the tunneling probability is evaluated across a range of interatomic distances, the importance of this latter point is apparent (figures 2(b) and (c)). For example, the D–D fusion rate predicted by the Gamow model for face-centered cubic palladium deuteride (PdD_x) has a range of more than 50 orders of magnitude depending on deuteron occupancy (see supplementary note S2.2). If only octahedral sites are occupied, the proximity-based fusion rate would be $< 10^{-120}/\text{s}$. This rate is increased to about $10^{-100}/\text{s}$ if both octahedral and tetrahedral sites are occupied. This would be further increased to $10^{-64}/\text{s}$ where D_2 accumulates in voids in the lattice (before considering screening effects). In PdD_x alloys, deuterium is known from neutron scattering experiments to favor octahedral site occupation, and vacancy formation and tetrahedral site occupation can occur at high concentration ($x > 0.9$) [31, 32–38]. Recent computational studies suggest that many $\text{M}(\text{H}/\text{D})_x$ alloys can form vacancies in the lattice capable of accommodating H_2/D_2 at high loading [39, 40]. It has also been proposed that sigma-bonded diderium molecules—a variant of regular D_2 molecules with different angular orientation—may be present in monovacancies at more modest loading [41, 42].

These considerations extend beyond proximity. The free electron density in Pd is $\sim 6.8 \times 10^{22} \text{ cm}^{-3}$, which corresponds to approximately one free electron per lattice atom [43]. The potential barrier between nearest-neighbor deuterons in a PdD_x alloy will be modified by this free electron density—a process known

as electron screening [44]. Simplistically, electron screening reduces the positive electrostatic repulsion between nuclei and results in a reduced interatomic distance (r_2-r_1) and is expressed as a reduction of $V(r)$ by a constant screening value (U_e) [44–48]. The two electrons in gas-phase D_2 correspond to a theoretical U_e value of ~ 20 eV [49, 50]. Theoretical values of U_e range from 50–150 eV for deuteron pairs in different metals [51, 52]. A U_e of 150 eV would correspond to a bond length reduction from 74 pm to 57 pm [53]. We calculate the effect of screening energies across this range (see supplementary note S2.3) for D–D fusion and find—in agreement with prior calculations [54]—that it is expected to provide an enhancement of fusion rates for D_2 upwards of 20 orders of magnitude in comparison to gas phase D_2 (figure 2(c)). This is qualitatively consistent with experimental observations from accelerator experiments [47, 51, 55]. However, quantitatively, experimental observations of fusion rates in solids appear to exceed theoretical estimates of U_e [47, 56]. Such discrepancies could be explained by local concentrations of electron density in the lattice (‘locally enhanced screening’ in figure 1), by dynamical increase of proximity and screening (‘fluctuations’ in figure 1), or by other enhancement mechanisms beyond the domain of atomic physics, as discussed in the following sections (‘internuclear resonances’ and ‘intranuclear resonances’ in figure 1).

Lattice imperfections such as impurities and defects lead to local changes in the electron band structure, which have been interpreted as a larger curvature of the electron valence band and thus as a larger effective electron mass m^* [57]. Since the screening potential U_e depends on the effective electron mass m^* , some lattice sites are then posited to provide for higher screening. Czernski *et al.* [58], referring to Zhang *et al* [59], argue that the effective electron mass m^* can locally be larger than the electron rest mass m_e by a factor of 9, corresponding to an increase of U_e by a factor of 3. This conjecture is consistent with accelerator experiments that suggest a U_e of 300 eV from the deuteron bombardment of vacancy-rich Zr, whereby the theoretically predicted U_e of pristine Zr is 112 eV [60]. However, a full phase space integration would be required to confirm this proposal. More details on locally enhanced screening are given in supplementary note S2.3.

The discussion so far only considers equilibrium conditions. In actuality, deuterium nuclei inside a metal lattice are dynamic [61–64]. The timescale discrepancy of atomic/electronic oscillations ($\gg 1$ fs) and fusion events ($\ll 1$ fs) is large. This discrepancy implies that short-lived extrema in atomic position and electron density are long from the perspective of two fusing nuclei. To account for dynamic atomic positions, the tunneling probability must be evaluated across all occurring proximities resulting from fluctuations [65]. Fluctuations are caused by factors such as lattice oscillations (phonons) or atomic diffusion and can cause temporary increases in proximity on the order of 5 pm over equilibrium values [65]. This change in interatomic distance corresponds to an expected enhancement of the D–D fusion rate of ~ 8 orders of magnitude (see supplementary note S2.4). Fluctuations in electron density are also relevant; it was recently proposed that the use of electronic fluctuations (plasmons) could temporarily increase electron density between deuterons in PdD_x , with a calculated increase in U_e of 40% [45, 46]. Such an increase would correspond to an enhancement of D–D fusion rates of ~ 15 orders of magnitude (see figure 2(c)).

To summarize, the atomic physics perspective contains mechanisms that will—non-contentiously and demonstrably—change fusion rates in the solid state: the effect of proximity as determined by equilibrium positions of hydrogen nuclei in their respective environments (site occupation); increased proximity caused by interactions of hydrogen nuclei with free electrons (electron screening); and further temporal enhancement of proximity (structural and electronic oscillations). These mechanisms manifest to differing degrees in any metal–deuterium system.

Our evaluation suggests that a fusion rate enhancement upwards of ~ 25 orders of magnitude can arise from such mechanisms without controversy.

Applying this enhancement to a fusion rate of 10^{-64} /s for D_2 at ambient temperature and pressure yields a fusion rate of 10^{-39} /s. This is ~ 20 orders of magnitude below the alleged ‘cold fusion’ rate of $\sim 10^{-23}$ /s. Some authors have argued that locally enhanced screening effects in the vicinity of lattice defect sites may further increase fusion rates by as much as another 15 orders of magnitude [58]. However, more research is needed to substantiate such conjectures.

In either case, when viewed exclusively through the lens of atomic physics, observable fusion at ambient conditions is not achievable.

3. The nuclear physics perspective

Nuclear physics frames fusion with more granularity than atomic physics. Here, nuclei are seen not as point masses and point charges but as objects with intranuclear structure [66]. The need for this increased granularity is apparent from empirical fusion data [67] (figure 3(a)). For example, proton–boron ($p-^{11}B$) fusion exhibits peaks of the reaction probability near 162 keV and 675 keV. Atomic physics alone cannot account for these peaks. The Gamow equation yields a smooth curve when reaction probabilities are evaluated as a function of energy [21]. Differences between reaction probabilities predicted by the Gamow

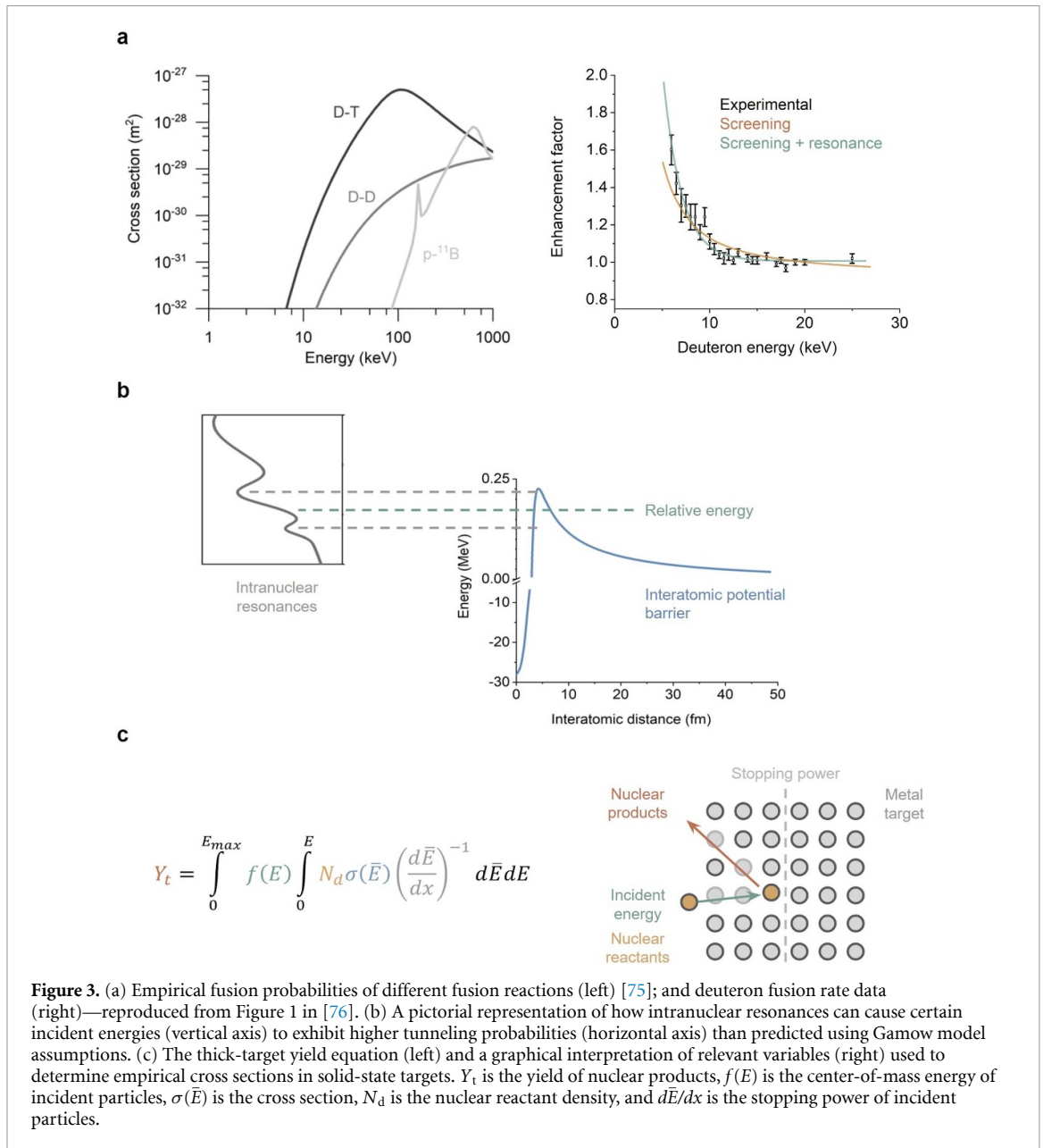


Figure 3. (a) Empirical fusion probabilities of different fusion reactions (left) [75]; and deuteron fusion rate data (right)—reproduced from Figure 1 in [76]. (b) A pictorial representation of how intranuclear resonances can cause certain incident energies (vertical axis) to exhibit higher tunneling probabilities (horizontal axis) than predicted using Gamow model assumptions. (c) The thick-target yield equation (left) and a graphical interpretation of relevant variables (right) used to determine empirical cross sections in solid-state targets. Y_t is the yield of nuclear products, $f(E)$ is the center-of-mass energy of incident particles, $\sigma(\bar{E})$ is the cross section, N_d is the nuclear reactant density, and $d\bar{E}/dx$ is the stopping power of incident particles.

model and empirical reaction probabilities are attributed to intranuclear structure that results from nucleon interactions [68, 69]. For p- ^{11}B fusion, the observed peaks originate from the resonant dynamics of the resulting $^8\text{Be} + ^4\text{He}$ nucleon clusters—a temporary molecule-like configuration of the twelve nucleons—which then rapidly disintegrates through sequential alpha decay into three ^4He nuclei [70]. For deuterium-tritium (D-T) fusion, a broad peak centered around 100 keV is attributed to a resonance associated with the polarized $3/2^+$ spin state of the resulting ^5He nucleus, which then disintegrates into a ^4He nucleus and a neutron [71]. Resonances—i.e., increased reaction probabilities at specific energies—occur when a particular configuration of nucleons can favorably accommodate a discrete amount of energy (figure 3(b)). Such conditions enable higher fusion rates if the energy imparted to the reactants is well-matched to their collective dynamics [72–74].

The p- ^{11}B and D-T resonances were not predicted, but measured. Several authors have sought to describe and predict intranuclear resonances on the basis of first-principles nuclear models [60, 71, 77, 78]. However, doing so is still aspirational due to the complexity of calculating nucleon-nucleon interactions [68, 69, 79–81]. This complexity can be divided into three challenges: (i) the strong nuclear force exhibits three-nucleon effects in addition to nucleon–nucleon effects; (ii) the strong nuclear force is strongly attractive between 1 fm and 2 fm, yet strongly repulsive at distances less than 1 fm; and (iii) the strong nuclear force is not organized around a center. Classical computations cannot easily handle these challenges

[82]. Accordingly, our understanding of intranuclear resonances is presently heavily dependent on what is experimentally accessible [67, 79, 80, 83].

No resonance has been experimentally detected for D–D fusion in the well-characterized *high-energy range* (10–1000 keV) [67] (figure 3(a)). The *medium-energy range* (5–10 keV) is less characterized for D–D fusion, but the sparse data reported suggest a fusion rate substantially higher than what is predicted by atomic physics considerations alone [47, 49, 52]. A hypothesis to explain unexpectedly high D–D fusion yields in the medium-energy range is the existence of a resonance for the resulting ^4He nucleus close to the reaction threshold near 23.85 MeV [60]. According to this hypothesis, the narrow maximum of this resonance would be in the *low-energy range* (<5 keV), with a tail that extends into the medium-energy range. Knowledge of such a putative resonance could then enable tuning of reactant energies to increase D–D fusion rates at low energy. A combination of theoretical considerations and comparisons with experimental data led Czerski and colleagues [60, 76] to predict resonance-based D–D fusion rate enhancement by 3–7 orders of magnitude in the eV range (see supplementary note S3.3 for a discussion of this predicted resonance and figure 3(a) for the experimental data used to motivate and calibrate it).

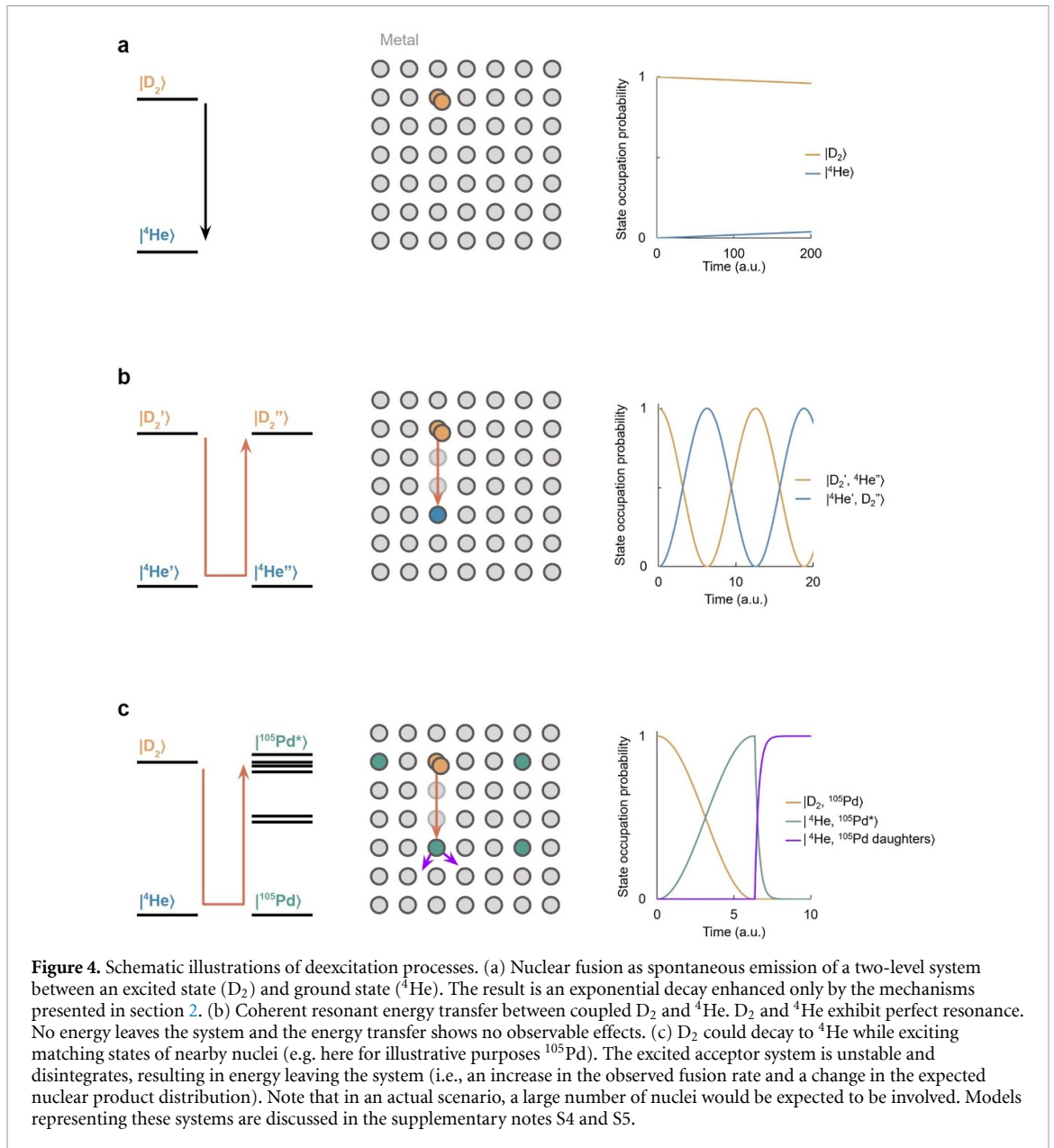
This hypothesis presents a clearly defined research issue, as there is limited published data for D–D fusion—or any fusion process—in the low-energy range (figure 3(a)). Moreover, the sparse data sets in this range are inconsistent between experiments for purportedly identical materials. Reliable <5 keV fusion rate data is necessary to develop low-energy fusion models required to verify or disprove the ^4He narrow-resonance hypothesis—and any other hypotheses related to the role of intranuclear structure at low and medium energies.

The sparsity of such data has a prosaic explanation that requires understanding how fusion rate measurements are performed and how reaction probabilities are calculated from the experimental data. Inconsistent data in prior work has been attributed to experimental challenges [49, 60, 84, 85]. Fusion rates are measured by accelerating particles (e.g., H^+ , D^+) into collision targets containing reactants (e.g., D, T, ^{11}B) and then detecting the resulting nuclear products (e.g., γ , n , ^4He , H^+). The fusion cross section $\sigma(\bar{E})$ —which corresponds to the fusion probability—is subsequently determined by solving the thick-target yield equation (figure 3(c)). Determination of $\sigma(\bar{E})$ requires measuring four Svariables: $d\bar{E}/dx$ (the stopping power of incident particles); Y_t (the yield of nuclear products); N_d (the nuclear reactant density), and $f(E)$ (the center-of-mass energy of incident particles). There are fundamental challenges for the determination of each variable for experiments in the low-energy range. $d\bar{E}/dx$ is on the same scale as most material passivation layers (<100 nm) [51]. Due to differences in materials processing, the passivation layer composition and thickness will vary between targets that are presumed identical [49, 85]. This implies that low-energy fusion experiments that appear identical may not be performed on the same material. Moreover, measurements of Y_t for low-energy experiments are weak enough to challenge the signal-to-noise limits of modern nuclear diagnostics [48, 51, 86]. Low observable fusion rates necessitate long experiments, which introduces the additional issue of N_d changing with time [49, 85]. Finally, many experimental setups measure a wide distribution of $f(E)$ values that make it difficult to identify narrow resonances [48, 51]. The consequence of these issues is sparse, inconsistent low-energy fusion rate data. If the role of intranuclear structure for low-energy fusion is to be clarified, experimental apparatus that enable total control of the variables within the thick-target yield equation must be developed.

To summarize, nuclear physics describes intranuclear resonances that demonstrably increase fusion rates at high energy (10–1000 keV) [67]. Similar resonances at low energy (<5 keV) are hypothesized to extend into the medium-energy range (5–10 keV) and account for unexpectedly high fusion rates observed in that range [47, 49, 52]. Due to the complexity of nuclear modeling, such hypotheses are presently only verifiable through the acquisition of low-energy fusion rate data [87]. Collection of reliable data sets at low energies is an unsolved challenge in experimental nuclear physics [48, 86]. Ambiguity about the role of intranuclear structure in low-energy fusion will remain until this challenge is met.

As concluded in section 2, the possibility of D–D fusion rates on the order of at least $10^{-39}/\text{s}$ —when considering D_2 in a palladium lattice with uniform electron screening at ambient conditions—is broadly accepted [51, 54, 88]. Additional application of the proposed intranuclear-resonance-based D–D fusion rate enhancement of 7 orders of magnitude then yields a rate of $10^{-32}/\text{s}$. When combined with the 15 orders of magnitude enhancement from locally increased screening at lattice defect sites, as also posited in Czerski 2022 [76] and discussed in section 2, an overall predicted fusion rate upwards of $10^{-19}/\text{s}$ results. This is positioned within range of alleged ‘cold fusion’ rates of $>10^{-23}/\text{s}$. However, more research is needed to discern whether the posited low-lying nuclear resonance of ^4He exists.

When viewed through the lens of both atomic physics and nuclear physics, observable fusion at ambient conditions is within the realm of possibilities.



4. The quantum dynamics perspective

Quantum dynamics—the study of evolving quantum systems as a function of time—frames nuclear fusion distinctly from atomic physics and nuclear physics. Here, fusion is treated as a quantum state transition rather than a quantum tunneling event⁴. From this viewpoint, a deuteron pair D_2 is an excited state of ${}^4\text{He}$ [89, 90]. The D–D reaction is represented by the D_2 four-nucleon cluster (i.e., the excited state) relaxing down to the more compact ${}^4\text{He}$ four-nucleon cluster (i.e., the ground state). The fusion rate is then equivalent to the state transition rate (figure 4(a)), and increasing the deexcitation rate corresponds to increasing the fusion rate.

Mechanisms for enhancing state transition rates have been described and experimentally demonstrated at both the atomic [91–95] and the nuclear level [96–100]. This acceleration occurs if excited atoms or nuclei are provided with alternative channels for deexcitation, which are faster than conventional channels. The fastest channels typically involve quantum coherence across interacting atoms or nuclei [101].

⁴ Note that a quantum state transition at the atomic level—such as a 2s to 1s transition in a hydrogen atom—is a hindered reconfiguration of electrons but still occurs with a mean probability (which is the half-life or state transition rate, akin to a tunneling rate). Similarly, a quantum state transition at the nuclear level—such as a 3/2- to 1/2- transition in a ${}^{57}\text{Fe}$ nucleus—is a reconfiguration of nucleons that is hindered but still occurs with a mean probability. A state transition from a higher energetic state to a lower one is a deexcitation with a rate associated with it (Γ).

Two classes of phenomena are at the heart of accelerated state transitions: the first one is *resonance energy transfer* (RET) [102, 103], a mechanism in which excitation energy is transferred nonradiatively from one system to another resonant or near-resonant system that is coupled. This means that the transfer of energy is achieved not through the radiative emission of a particle carrying the excitation energy, but through the coupling of both systems to a common field. The electromagnetic field is an example of such a field. At the atomic level, this mechanism is widely known and exploited in biology and chemistry (FRET experiments) [104]. Nonradiative energy transfer is conventionally believed to play a much less prominent role at the nuclear level because of the weakness of couplings that affect nuclear energetic states, compared to their much larger state transition energies. However, these weak couplings can be increased under particular circumstances (see box 1). Nonradiative transfer of nuclear energy has been theoretically described and experimentally emulated with precisely engineered resonant cavities [100, 105–109].

The second mechanism to accelerate deexcitation is *superradiance*, also known by the more general term *Dicke enhancement* [110]. This is a phenomenon that can occur when N excited emitters are coupled together, which then deexcite at a rate that depends on N (and is in some configurations proportional to N^2). For large N , this can be substantially faster than the typical exponential decay from spontaneous emission [98, 99]. In recent experiments, multiple ^{57}Fe nuclei were collectively excited by an x-ray free-electron laser [96]. The affected nuclei comprised a quantum system in superposition that was able to absorb and emit nuclear excitation collectively. An acceleration proportional to the number of excited nuclei has been experimentally observed for the deexcitation of the first excited state of ^{57}Fe nuclei [96], following the dynamics predicted for atoms by Dicke in 1954 [110] and for nuclei by Terhune and Baldwin in 1965 [111]. These studies empirically demonstrate that nuclear decay can be manipulated and accelerated through quantum coherent effects in the solid state.

RET and Dicke enhancement can be combined: when a large number of atoms or nuclei N participate in a coherently coupled quantum system within which RET occurs, then transfer can be accelerated by an enhancement factor up to N^2 [112]. This acceleration of transfer follows directly from the application of canonical quantum dynamics models—such as the well-known Dicke model [113]—to the configuration of coupled quantum systems described above (see supplementary note S4 and S5). Dicke-enhanced RET is referred to as *supertransfer* and has been experimentally demonstrated at the atomic level [114, 115]. Related mechanisms such as loss-based acceleration of transfer can provide further enhancement [116, 117]. Supertransfer is expected to also manifest in excitation transfer at the nuclear level [99, 109].

An increased deuterium fusion rate for molecular D_2 in a metal lattice that results from accelerated nuclear state transitions is predicted by a corresponding Dicke model if: (i) a coupling—even if weak—exists between nuclear states of nearby nuclei via common oscillator modes; (ii) coupled acceptor nuclei exhibit states that are well-matched to the energy held by the D_2 donor state ($\sim 23,848,109$ eV); and (iii) the system evolves coherently with large Dicke enhancement factors [118]. A precise match for the D_2 donor state is a coupled ^4He nucleus, as it is capable of accommodating the energy released in the $|\text{D}_2\rangle \rightarrow |^4\text{He}\rangle$ transition resonantly through the complementary $|^4\text{He}\rangle \rightarrow |\text{D}_2\rangle$ transition [119]. In the presence of coupling and substantial supertransfer enhancement (figure 4(b)), accelerated deexcitation $|\text{D}_2\ ^4\text{He}\rangle \rightarrow |^4\text{He}\ \text{D}_2\rangle$ is predicted, when applying the established Dicke model to this configuration. This process would manifest as nonlinear occupation probability oscillations between two population states, i.e., nonlinear Rabi oscillations (see supplementary note S5). The maximum transfer rate for this process is estimated to be faster than the $|\text{D}_2\rangle \rightarrow |^4\text{He}\rangle$ spontaneous emission rate (based on the incoherent tunneling probability in the Gamow model)—see supplementary note S5.

If energy redistribution is limited to remain within a coherent closed quantum system, then it is experimentally difficult to be detected and practically not exploitable. In the example above, every accelerated (exothermic) fusion event $|\text{D}_2\rangle \rightarrow |^4\text{He}\rangle$ would be offset by a matching (endothermic) fission event $|^4\text{He}\rangle \rightarrow |\text{D}_2\rangle$ with all energy remaining within the closed system. However, if acceptor nuclei disintegrate before the next transfer, the closed quantum system becomes open, with energy leaving in the form of energetic particles (figure 4(c)). In a metal-deuterium lattice with impurities, many common nuclei exhibit a dense number of excited states in the higher MeV range and represent acceptor candidates for nuclear RET processes (see supplementary note S5.4). Transferring to heavier nuclei than ^4He can involve less hundred acceptor states, making the process faster (see supplementary note S5.5 ff.). And with many available states, many different secondary reactions become possible, depending on exact conditions. For instance, upon receiving a large quantum of energy, some nuclei would promptly disintegrate through nuclear emission processes (^4He , H^+ , n , γ). The result would be nuclear products, and a variety of such products based on the identity of available impurities—as is suggested by certain experimental reports [14–16, 19] (see supplementary note S1.3). This implies that rigorous fusion research in solid-state materials may necessitate purity requirements as well as deliberate doping similar to the semiconductor industry [120].

If acceptor nuclei are present in such a coupled system that can absorb the donor energy as a group, then RET to multiple acceptor nuclei becomes possible, as long as the donor energy matches the sum of acceptor energies [118] (see supplementary note S5.7 ff.). The conversion of large energy quanta into multiple smaller quanta is known as downconversion [121, 122].

To summarize, quantum dynamics offers mechanisms for increasing state transition rates at both the atomic and nuclear levels. Acceleration of atomic [91–95] and nuclear [96–99] state transitions has been described and demonstrated. Treatment of nuclear fusion as a quantum state transition provides underexplored handles for fusion rate enhancement. RET mediated by interactions between nuclear states and oscillator modes available in the lattice, enhanced by supertransfer effects, are candidate phenomena for increasing fusion rates in the solid state. For the situations considered above—D₂ coherently coupled to resonant acceptor nuclei (figures 4(b) and (c))—the relative change in the D–D fusion rate has been estimated, resulting in an increase upwards of 30 orders of magnitude (see supplementary note S5). Application of this enhancement to the (unscreened) baseline spontaneous fusion rate of ambient deuterium at 10^{−64}/s yields a fusion rate estimate of about 10^{−34}/s. Adding a Pd screening potential to the calculation, per the discussion in section 2, yields a fusion rate of >10^{−14}/s. This is positioned within range of alleged ‘cold fusion’ rates of >10^{−23}/s. Note that these numbers derive from an idealized model that emphasizes conceptual simplicity (per supplementary note S5.5)—a more detailed technical treatment, which explicitly takes into account the need of transfer rates to exceed conservative decoherence times, arrives at even higher numbers and is provided in supplementary notes S5.8 ff.

When viewed through the lens of both atomic physics and quantum dynamics, observable fusion at ambient conditions is within the realm of possibilities.

Questions remain to what extent this theoretically predicted mechanism does indeed lead to observable outcomes. For significant effects, excited states of lattice nuclei would—individually or collectively—need to be close to the 23.85 MeV transition energy of the |D₂⟩ → |⁴He⟩ transition since the transfer probability decreases rapidly with deviation from resonance. Moreover, the lifetimes of such states would need to be sufficiently long to participate in coherent dynamics [123] (supplementary note S5.4 and S5.8). What excited states are available in lattice nuclei, and what their energy levels and lifetimes are, has not been comprehensively charted, but can be predicted, e.g., based on liquid drop model calculations [123–125] (supplementary note S5.4). As for long lifetimes, some nuclear cluster states are known to be comparatively stable. Moreover, the coherence domain would need to be sufficiently large and long-lived to provide substantial Dicke enhancement factors and transfer rates (supplementary note S5.8).

To study the robustness of Dicke-enhanced nuclear excitation transfer in practice we suggest exploring the phenomenon based on simpler basic science experiments such as a modified Chumakov experiment [96], where—instead of exploiting superradiance—the delocalized 14.4 keV excitation of ⁵⁷Fe is transferred to other ⁵⁷Fe nuclei. This would have the advantage of having perfectly resonant receiver nuclei available as well as a comparatively small transition energy, both of which would ease the demands on coupling strengths and the size and lifetime of the coherence domain.

Box 1. Interactions between nuclei

Quantum systems such as atoms or nuclei can interact with one another through fundamental forces and form superposition states that can redistribute energy. Interactions can be mediated by oscillators, which are treated as shared quantum fields. The extent to which such interactions manifest (i.e., the coupling strength) determines the rates of induced dynamics (e.g., ⁵⁷Fe* → ⁵⁷Fe + γ).

Interactions between nuclei are canonically weak compared to interactions between atoms. At the atomic level, dominant interactions originate from the antenna-like nature of atomic dipoles. Comparable interactions exist at the nuclear level but are weaker due to the small dipole of nuclei. Electromagnetic interactions between atoms can be on the order of 50 meV (e.g., photosynthesis [126, 127]) and between nuclei they are on the order of 0.1 neV (e.g., nuclear magnetic resonance [128, 129]).

Both nuclear and atomic interactions can be driven by external stimulation. For example, at the atomic level, the coupling between phonons and superconducting qubits can be increased by expanding the phonon population in a phononic cavity [130]. At the nuclear level, magnon-nuclear coupling can be increased by an external radio frequency (RF) field and by internal magnetic fields, whereby the induced coupling scales with the field strength [131, 132]. Internal magnetic fields can be activated via the stimulation of phonons and spin waves [133]. For both phonon-qubit and magnon-nuclear systems,

coupling strengths of 100 neV are typical [93, 131]. Some examples for undriven and driven couplings at the atomic level and the nuclear level are shown below:

	Undriven	Driven
Atomic level	Electric dipole–dipole coupling between molecules (e.g. between chlorophylls in photosynthesis). Coupling strength: ~ 50 meV [134]	Phonon-qubit coupling (e.g. a phononic cavity as a quantum bus between superconducting circuits). Coupling strength: ~ 100 neV [130]
Nuclear level	Magnetic dipole–dipole coupling between nuclei (e.g. between C nuclei in ^{13}C NMR measurements). Coupling strength: < 0.1 neV [135]	Magnon-nuclear coupling (e.g. ^{57}Fe nuclei interacting with an RF field). Coupling strength: ~ 100 neV [131]

Phonon–nuclear coupling is suggested to be larger still and also externally driven [136]. The coupling originates from the center-of-mass contribution to nucleon motion resulting from lattice oscillations [136]. This contribution represents a boost to the nuclear spin-orbit coupling, which affects nuclear states. Coupling strength estimates for ^{181}Ta nuclei interacting with a 10 THz field are on the order of meV [137].

5. Conclusion

Within the three major communities presented—atomic physics, nuclear physics, and quantum dynamics—mechanisms are known that increase nuclear fusion rates in solid-state materials. No individual mechanism appears to traverse the > 40 orders of magnitude necessary to make solid-state fusion at ambient conditions technologically relevant. A combination of them might.

This final claim is only useful if it leads to testable hypotheses. Consider D–D fusion in PdD_x through the perspective of the three fields discussed above. Considerations from the atomic physics perspective necessitate that D_2 exists in the lattice. This insight provides a clear research target to pursue for solid-state fusion studies—vacancy-rich PdVac_yD_x that can accommodate D_2 . This target can be pursued without contention, as vacancy-rich metal–hydrogen alloys are of interest to multiple communities. Nuclear physics suggests that anomalously high D–D fusion rates at low energy (< 5 keV) could be explained by intranuclear resonances centered in the < 1 keV range. Highly controlled D–D fusion rate measurements in that energy range would provide clarification. The challenges associated with collection of such data are firmly in the domain of materials science and nuclear diagnostics, and would benefit from collaboration between chemists and physicists. This gives a clear research target to pursue—the development of experimental apparatus for the collection of high resolution D–D fusion data in the < 5 keV range. Again, this pursuit advances our understanding of nuclear physics and can be done without contention, as such data contributes to nuclear model development. Quantum dynamics suggests possible mechanisms of significantly increasing nuclear reaction rates in the solid state through quantum coherent effects. Mechanisms such as superradiance have been empirically demonstrated to accelerate nuclear state transitions while supertransfer has been demonstrated to occur at the atomic level. The question whether supertransfer can occur at the nuclear level follows naturally. This gives a clear research target to pursue—fabrication of materials with controlled quantities of donor nuclei (e.g., $^{57}\text{Fe}^*$) and controlled quantities of resonant or near-resonant acceptor nuclei, and subsequent study of nuclear state changes in these materials under coherent stimulation (e.g. via phonons, plasmons, or magnons). Such studies could ideally be expanded to include vacancy-rich materials with high deuterium loading that also benefit from proximity and screening enhancements (e.g. PdVac_yD_x with $x > 0.9$ and $y > 0.01$), as discussed in section 2, taking advantage of multiple enhancement mechanisms. Experiments with reports of unexpected nuclear products from low-energy stimulation of metal–hydrogen samples [14–19, 138] may in principle have matched these criteria, but well-controlled and well-characterized investigations of such systems are lacking. If the presented mechanisms are indeed behind the experimental reports of energetic particle emission from stimulated metal–hydrogen systems at ambient conditions, the technological implications would be substantial. This pertains most immediately to fusion technology development but may extend to other areas of nuclear engineering such as nuclear isotope production.

Observable fusion at ambient conditions—when viewed through the lens of atomic physics, nuclear physics, and quantum dynamics—is a research subject of interest.

The research targets above cross multiple scientific disciplines. Research of fusion in solid-state environments requires no sacrifice when it is recognized as a question that will be asked and answered through the advancement of established fields. We call on the scientific community to explore the mechanisms described here—individually and in conjunction with one another—to push the frontier of physics into unexplored territory. If the possibility of technologically relevant fusion in the solid state cannot be readily precluded within the framework of known physics, then we have a societal obligation to explore it.

Data availability statement

All data that support the findings of this study are included within the article (and any supplementary files).

Author contributions

F M conceived the article and wrote the first draft, drawing on ideas developed by P L H over time. All authors discussed the article. C H revised the atomic and nuclear physics sections and created the figures with F M. P L H and N G revised the atomic physics and quantum dynamics section. N G and F M supervised the process.

Acknowledgments

We would like to thank Matt Lilley, Jonah Messinger, Sadie Forbes, Matt Trevithick, Ross Koningstein, David Fork, Yet-Ming Chiang, Jeremy Munday, Thomas Schenkel, Curtis Berlinguette, Konrad Czerski, Robert Duncan, Huw Price, Mingda Li, Carlotta Barone-MacDonald, Hana Assouz, Steven Byrnes, and Jonas Karthein for helpful discussions. Support from Google and the Anthropocene Institute is gratefully acknowledged.

Funding information

This work was partially supported by Google (F M, C H) and the Anthropocene Institute (F M, N G).

ORCID iDs

Florian Metzler  <https://orcid.org/0000-0003-1818-1332>

Nicola Galvanetto  <https://orcid.org/0000-0002-0408-1747>

References

- [1] Adams J B 1966 A review of nuclear fusion research *Proc. Phys. Soc.* **89** 189–216
- [2] Rose D J 1969 Engineering feasibility of controlled fusion: a review *Nucl. Fusion* **9** 183–203
- [3] Clark J and MacKerron G 1989 Great expectations: a review of nuclear fusion research *Energy Policy* **17** 49–56
- [4] Rebut P-H 1995 ITER: the first experimental fusion reactor *Fusion Eng. Des.* **30** 85–118
- [5] Shimomura Y and Spears W 2004 Review of the ITER project *IEEE Trans. Appl. Supercond.* **14** 1369–75
- [6] Fleischmann M and Pons S 1989 Electrochemically induced nuclear fusion of deuterium *J. Electroanal. Chem. Int. Electrochem.* **261** 301–8
- [7] Jones S E, Palmer E P, Czirr J B, Decker D L, Jensen G L, Thorne J M, Taylor S F and Rafelski J 1989 Observation of cold nuclear fusion in condensed matter *Nature* **338** 737–40
- [8] Browne M W 1989 *Fusion in a jar: chemists' claim ignites an uproar* (NY Times) p 28
- [9] Miskelly G M, Heben M J, Kumar A, Penner R M, Sailor M J and Lewis N S 1989 Analysis of the published calorimetric evidence for electrochemical fusion of deuterium in palladium *Science* **246** 793–6
- [10] Albagli D et al 1990 Measurement and analysis of neutron and gamma-ray emission rates, other fusion products, and power in electrochemical cells having Pd cathodes *J. Fusion Energy* **9** 133–48
- [11] Huizenga J R 1992 *Cold Fusion: The Scientific Fiasco of the Century* vol 81 (Univ. of Rochester Press)
- [12] Leggett A J and Baym G 1989 Can solid-state effects enhance the cold-fusion rate? *Nature* **340** 45–46
- [13] Goodstein D 1994 Pariah science: whatever happened to cold fusion? *Am. Sch.* **63** 527–41 (available at: www.jstor.org/stable/41212118)
- [14] Takahashi A, Takeuchi T, Iida T and Watanabe M 1990 Emission of 2.45 MeV and higher energy neutrons from D₂O-Pd cell under biased-pulse electrolysis *J. Nucl. Sci. Technol.* **27** 663–6
- [15] Chambers G P, Eridon J E, Grabowski K S, Sartwell B D and Chrisey D B 1990 Charged particle spectra of palladium thin films during low energy deuterium ion implantation *J. Fusion Energy* **9** 281–5
- [16] Chambers G P, Hubler G K and Grabowski K S 1991 Search for Energetic Charged Particle Reaction Products during Deuterium Charging of Metal Lattices *AIP Conf. Proc.* **228** 383–96
- [17] Menlove H O, Fowler M M, Garcia E, Miller M C, Paciotti M A, Ryan R R and Jones S E 1990 Measurement of neutron emission from Ti and Pd in pressurized D₂ gas and D₂O electrolysis cells *J. Fusion Energy* **9** 495–506
- [18] Belyukov I L, Bondarenko N B, Janelidze A A, Gapanov M Y, Griбанov K G, Kondratov S V, Maltsev A G, Novikov P I, Tsvetkov S A and Zakharov V I 1991 Laser-induced cold nuclear fusion in Ti-H₂-D₂-T₂ compositions *Fusion Technol.* **20** 234–8

- [19] Ziehm E 2022 An experimental investigation of low energy nuclear reactions in a DC glow discharge *Diss.* University of Illinois at Urbana-Champaign
- [20] Koonin S E and Nauenberg M 1989 Calculated fusion rates in isotopic hydrogen molecules *Nature* **339** 690
- [21] Gamow G 1928 Zur Quantentheorie des Atomkernes *Z. Phys.* **51** 204–12
- [22] Frost A A and Musulin B 1954 Semiempirical potential energy functions. I. The H_2 and H_2^+ diatomic molecules *J. Chem. Phys.* **22** 1017–20
- [23] Jones J E 1924 On the determination of molecular fields.—I. From the variation of the viscosity of a gas with temperature *Proc. R. Soc. A* **106** 441–62
- [24] Lennard-Jones J E 1924 On the determination of molecular fields. II. From the equation of state of gas *Proc. R. Soc. A* **106** 463–77
- [25] Jones J E and Chapman S 1924 On the determination of molecular fields. III.—From crystal measurements and kinetic theory data *Proc. R. Soc. A* **106** 709–18
- [26] Saha R, Markmann A and Batista V S 2012 Tunneling through Coulombic barriers: quantum control of nuclear fusion *Mol. Phys.* **110** 995–9
- [27] Dunlap R A A and Dunlap R A 2021 *Energy from Nuclear Fusion* (IOP Publishing)
- [28] Roepke G and Baird J C 1989 Fluctuation of the deuteron pair distribution function in a charged particle system and the fusion cross section in solids *Proc. of the 19th Int. Symp. on Nuclear Physics: Nuclear Processes in Fusion Reactors (6–10 November 1989)* ZFK-733
- [29] Guo H et al 2020 Innovative approaches towards an economic fusion reactor *Natl Sci. Rev.* **7** 245–7
- [30] Harrison W A 1972 The theory of interatomic potentials in solids *Interatomic Potentials and Simulation of Lattice Defects ed* P C Gehlen, J R Beeler and R I Jaffee (Springer) pp 69–90
- [31] Flanagan T B and Oates W A 1991 The palladium-hydrogen system *Annu. Rev. Mater. Sci.* **21** 269–304
- [32] Fukai Y and Ōkuma N 1994 Formation of superabundant vacancies in Pd hydride under high hydrogen pressures *Phys. Rev. Lett.* **73** 1640–3
- [33] Fukai Y 1995 Formation of superabundant vacancies in metal hydrides at high temperatures *J. Alloys Compd.* **231** 35–40
- [34] Fukai Y, Ishii Y, Goto Y and Watanabe K 2000 Formation of superabundant vacancies in Pd–H alloys *J. Alloys Compd.* **313** 121–32
- [35] Fukumuro N, Fukai Y, Sugimoto H, Ishii Y, Saitoh H and Yae S 2020 Superstoichiometric hydride PdH_x ≤ 2 formed by electrochemical synthesis: dissolution as molecular H₂ proposed *J. Alloys Compd.* **825** 153830
- [36] Worsham J, Wilkinson M and Shull C 1957 Neutron-diffraction observations on the palladium-hydrogen and palladium-deuterium systems *J. Phys. Chem. Solids* **3** 303–10
- [37] Ferguson G A, Schindler A I, Tanaka T and Morita T 1965 Neutron Diffraction Study of Temperature-Dependent Properties of Palladium Containing Absorbed Hydrogen *Phys. Rev.* **137** A483–A487
- [38] Kofu M, Hashimoto N, Akiba H, Kobayashi H, Kitagawa H, Tyagi M, Faraone A, Copley J R, Lohstroh W and Yamamuro O 2016 Hydrogen diffusion in bulk and nanocrystalline palladium: A quasielastic neutron scattering study *Phys. Rev. B* **94**
- [39] Zhang C and Alavi A 2005 First-principles study of superabundant vacancy formation in metal hydrides *J. Am. Chem. Soc.* **127** 9808–17
- [40] Nazarov R, Hickel T and Neugebauer J 2014 *Ab initio* study of H-vacancy interactions in fcc metals: implications for the formation of superabundant vacancies *Phys. Rev. B* **89** 144108
- [41] Hagelstein P L and Chaudhary I U 2009 Arguments for diderium near monovacancies in PdD *15th Int. Conf. on Condensed Matter Nuclear Science (5–9 October 2009, Rome, Italy)* pp 282–7
- [42] Hagelstein P L 2014 Molecular D₂ near vacancies in PdD and related problems *J. Condens. Matter Nucl. Sci.* **13** 138–48
- [43] Horowitz C J 1989 Cold nuclear fusion in metallic hydrogen and normal metals *Phys. Rev. C* **40** 1555–8
- [44] Raiola F et al 2006 Electron screening: a review *AIP Conf. Proc.* **831** 296–303
- [45] Fork D K, Munday J N, Narayan T and Murray J B 2019 *Target structure for enhanced electron screening* 10,264,661
- [46] Fork D K, Munday J N, Narayan T and Murray J B 2020 *Enhanced electron screening through plasmon oscillations* 10,566,094
- [47] Czernski K, Huke A, Biller A, Heide P, Hoefl M and Ruprecht G 2001 Enhancement of the electron screening effect for d + d fusion reactions in metallic environments *EPL* **54** 449–55
- [48] Huke A, Czernski K and Heide P 2003 Experimental techniques for the investigation of the electron screening effect for d d fusion reactions in metallic environments *Nucl. Phys. A* **719** C279–82
- [49] Huke A, Czernski K and Heide P 2007 Measurement of the enhanced screening effect of the d+d reactions in metals *Nucl. Instrum. Methods Phys. Res. B* **256** 599–618
- [50] Shoppa T D, Koonin S E, Langanke K and Seki R 1993 One- and two-electron atomic screening in fusion reactions *Phys. Rev. C* **48** 837–40
- [51] Huke A, Czernski K, Heide P, Ruprecht G, Targosz N and Żebrowski W 2008 Enhancement of deuteron-fusion reactions in metals and experimental implications *Phys. Rev. C* **78** 015803
- [52] Targosz-Ślęczka N, Czernski K, Huke A, Ruprecht G, Weissbach D, Martin L, Kiliç A I, Kaczmarek M and Winter H 2013 Experiments on screening effect in deuteron fusion reactions at extremely low energies *Eur. Phys. J. Spec. Top.* **222** 2353–9
- [53] Vaselli M, Harith M A, Palleschi V, Salvetti G and Singh D P 1989 Screening effect of impurities in metals: a possible explanation of the process of cold nuclear fusion *Nuovo Cimento C* **11** 927–32
- [54] Prados-Estévez F M, Subashiev A V and Nee H H 2017 Nuclear fusion by lattice confinement *J. Phys. Soc. Japan* **86** 074201
- [55] Czernski K, Huke A, Heide P and Ruprecht G 2006 Experimental and theoretical screening energies for the 2H(d, p)3H reaction in metallic environments *Eur. Phys. J. A* **27** 83–88
- [56] Spitaleri C, Bertulani C A, Fortunato L and Vitturi A 2016 The electron screening puzzle and nuclear clustering *Phys. Lett. B* **755** 275–8
- [57] Kittel C and McEuen P 2018 *Introduction to Solid State Physics* (Wiley)
- [58] Czernski K, Targosz-Ślęczka N and Kaczmarek M 2020 Deuteron–deuteron reaction cross sections at very low energies *Acta Phys. Pol. B* **51** 649
- [59] Zhang J, McIlroy D N and Dowben P A 1995 Correlation between screening and electron effective mass across the nonmetal-metal transition in ultrathin films *Phys. Rev. B* **52** 11380
- [60] Czernski K, Weissbach D, Kiliç A I, Ruprecht G, Huke A, Kaczmarek M, Targosz-Ślęczka N and Maass K 2016 Screening and resonance enhancements of the 2H(d, p)3H reaction yield in metallic environments *EPL* **113** 22001
- [61] Gillan M J 1986 A simulation model for hydrogen in palladium. I. Single-particle dynamics *J. Phys. C: Solid State Phys.* **19** 6169
- [62] Gillan M J 1987 A simulation model for hydrogen in palladium. II. Mobility and thermotransport *J. Phys. C: Solid State Phys.* **20** 521

- [63] Narayan T C, Hayee F, Baldi A, Leen Koh A, Sinclair R and Dionne J A 2017 Direct visualization of hydrogen absorption dynamics in individual palladium nanoparticles *Nat. Commun.* **8** 14020
- [64] Kofu M and Yamamuro O 2020 Dynamics of atomic hydrogen in palladium probed by neutron spectroscopy *J. Phys. Soc. Japan* **89** 051002
- [65] Koonin S E 1989 Enhancement of Cold Fusion Rates by Fluctuations NSF-ITP-89-55
- [66] Takigawa N and Washiyama K 2017 *Fundamentals of Nuclear Physics* (Springer)
- [67] Zerkin V V and Pritychenko B 2018 The experimental nuclear reaction data (EXFOR): extended computer database and web retrieval system *Nucl. Instrum. Methods Phys. Res. A* **888** 31–43
- [68] Quaglioni S, Navr P, Roth R and Horiuchi W 2012 From nucleons to nuclei to fusion reactions *J. Phys.: Conf. Ser.* **402** 012037
- [69] Nazarewicz W 1998 Nuclear structure at the limits *11th Physics Summer School on Frontiers in Nuclear Physics: From Quark-Gluon Plasma to Supernova (Canberra, Australia, 12–23 January 1998)*
- [70] Geser F A and Valente M 2020 A theoretical model for the cross section of the proton-boron fusion nuclear reaction *Radiat. Phys. Chem.* **167** 108224
- [71] Hupin G, Quaglioni S and Navrátil P 2019 *Ab initio* predictions for polarized deuterium-tritium thermonuclear fusion *Nat. Commun.* **10** 1–8
- [72] Bethe H A and Placzek G 1937 Resonance effects in nuclear processes *Phys. Rev.* **51** 450–84
- [73] MacDonald W and Mekjian A 1967 Fine structure in nuclear resonances *Phys. Rev.* **160** 730–9
- [74] Giacomelli G 2013 *Total Cross-Section Measurements: Progress in Nuclear Physics* (Elsevier)
- [75] Chadwick M B, Herman M, Obložinský P, Dunn M E, Danon Y, Kahler A C, Smith D L, Pritychenko B, Arbanas G and Arcilla R 2011 ENDF/B-VII. 1 nuclear data for science and technology: Cross sections, covariances, fission product yields and decay data *Nuclear Data Sheets* **112** 2887–996
- [76] Czernski K 2022 Deuteron-deuteron nuclear reactions at extremely low energies *Phys. Rev. C* **106** L011601
- [77] Shirokov A M, Papadimitriou G, Mazur A, Mazur I, Roth R and Vary J 2016 Prediction for a four-neutron resonance *Phys. Rev. Lett.* **117** 182502
- [78] Schieck H P G 2014 *Nuclear Reactions: An Introduction* (Springer)
- [79] Sobczewski A and Litvinov Y A 2014 Predictive power of nuclear-mass models *Phys. Rev. C* **90** 017302
- [80] Mendoza-Temis J, Morales I, Barea J, Frank A, Hirsch J G, Vieira J C L, Van Isacker P and Velázquez V 2008 Testing the predictive power of nuclear mass models *Nucl. Phys. A* **812** 28–43
- [81] Krane K S and Halliday D 1987 *Introductory Nuclear Physics* (John Wiley & Sons)
- [82] Luu T and Walker-Loud A 2009 Nuclear forces and high-performance computing: the perfect match *J. Phys.: Conf. Ser.* **180** 11
- [83] Kaczmarek M, Czernski K, Weissbach D, Kilic A I, Ruprecht G and Huke A 2017 Threshold resonance contribution to the thick target $2\text{H}(\text{d}, \text{p})3\text{H}$ reaction yield *Acta Phys. Pol. B* **48** 489–93
- [84] Huke A 2002 Die Deuteronen-Fusionsreaktionen in Metallen. *Diss. Technische Universität Berlin*
- [85] Czernski K, Huke A, Martin L, Targosz N, Blauth D, Górka A, Heide P and Winter H 2007 Measurements of enhanced electron screening in $\text{d}+\text{d}$ reactions under UHV conditions *J. Phys. G: Nucl. Part. Phys.* **35** 014012
- [86] Kilic A I and Kustan F K 2019 Material-dependent $\text{d}+\text{d}$ cross-section in dense and metallic mesh wire environments at very low energies *Mod. Phys. Lett. A* **34** 1950234
- [87] Berlinguette C P, Chiang Y-M, Munday J N, Schenkel T, Fork D K, Koningstein R and Trevithick M D 2019 Revisiting the cold case of cold fusion *Nature* **570** 45–51
- [88] Pines V et al 2020 Nuclear fusion reactions in deuterated metals *Phys. Rev. C* **101** 044609
- [89] Schwinger J 1990 Nuclear energy in an atomic lattice. 1 *Z. Phys. D: At., Mol. Clusters* **15** 221–25
- [90] Schwinger J 1991 Nuclear energy in an atomic lattice—causal order *Progr. Theoret. Phys.* **85** 711–2
- [91] Kaur M, Kaur P, Sahoo B K and Arora B 2018 Dynamics of resonant energy transfer in one-dimensional chain of Rydberg atoms *Eur. Phys. J. D* **72** 150
- [92] Brekke E 2009 Stimulated emission studies of ultracold Rydberg atoms *Diss. University of Wisconsin–Madison* (<https://doi.org/10.1007/s11605-009-0884-9>)
- [93] Newman W D, Cortes C L, Afshar A, Cadien K, Meldrum A, Fedosejevs R and Jacob Z 2018 Observation of long-range dipole-dipole interactions in hyperbolic metamaterials *Sci. Adv.* **4** eaar5278
- [94] Scheibner M, Schmidt T, Worschech L, Forchel A, Bacher G, Passow T and Hommel D 2007 Superradiance of quantum dots *Nat. Phys.* **3** 106–10
- [95] Wang T, Yelin S F, Côté R, Eyler E E, Farooqi S M, Gould P L, Kostrun M, Tong D and Vrinceanu D 2007 Superradiance in ultracold Rydberg gases *Phys. Rev. A* **75** 033802
- [96] Chumakov A I et al 2017 Superradiance of an ensemble of nuclei excited by a free electron laser *Nat. Phys.* **14** 261–4
- [97] Metzler F 2019 Experiments to Investigate Phonon-Nuclear Interactions *Thesis Massachusetts Institute of Technology*
- [98] Kravvaris K and Volya A 2017 Quest for superradiance in atomic nuclei *AIP Conf. Proc.* **1912** 020010
- [99] Shen T-X 1991 Superradiance and Subradiance in Systems of Excited Nuclei *Thesis Rice University*
- [100] Haber J, Kong X, Strohm C, Willing S, Gollwitzer J, Bocklage L, Rüffer R, Pálffy A and Röhlberger R 2017 Rabi oscillations of x-ray radiation between two nuclear ensembles *Nat. Photon.* **11** 720–5
- [101] Metzler F, Sandoval J I and Galvanetto N 2023 The emergence of quantum energy science *J. Phys. Energy* **5** 041001
- [102] Andrews D L 2009 *Resonance Energy Transfer: Theoretical Foundations and Developing Applications* (SPIE Press)
- [103] Jones G A and Bradshaw D S 2019 Resonance energy transfer: from fundamental theory to recent applications *Front. Phys.* **7** 100
- [104] Nettels D, Galvanetto N, Ivanović M T, Nüesch M, Yang T and Schuler B 2024 Single-molecule FRET for probing nanoscale biomolecular dynamics *Nat. Rev. Phys.* **6** 587–605
- [105] Suhl H 1958 Effective nuclear spin interactions in ferromagnets *Phys. Rev.* **109** 606
- [106] Nakamura T 1958 Indirect coupling of nuclear spins in antiferromagnet with particular reference to MnF_2 at very low temperatures *Prog. Theor.* **20** 542–52
- [107] Rubinstein M 1999 Exchange coupling between two magnetic films separated by an antiferromagnetic spacer *J. Appl. Phys.* **85** 5880–2
- [108] Shiomi Y, Lustikova J, Watanabe S, Hirobe D, Takahashi S and Saitoh E 2018 Spin pumping from nuclear spin waves *Nat. Phys.* **15** 22–26
- [109] Hagelstein P L 2018 Phonon-mediated nuclear excitation transfer *J. Condens. Matter Nucl. Sci.* **27** 97–142
- [110] Dicke R H 1954 Theory of superradiance *Phys. Rev.* **93** 99–110
- [111] Terhune J H and Baldwin G C 1965 Nuclear superradiance in solids *Phys. Rev. Lett.* **14** 589–91

- [112] Lloyd S and Mohseni M 2010 Symmetry-enhanced supertransfer of delocalized quantum states *New J. Phys.* **12** 075020
- [113] Roses M M and Dalla Torre E G 2020 Dicke model *PLoS One* **15** e0235197
- [114] Abasto D F, Mohseni M, Lloyd S and Zanardi P 2012 Exciton diffusion length in complex quantum systems: the effects of disorder and environmental fluctuations on symmetry-enhanced supertransfer *Phil. Trans. R. Soc. A* **370** 3750–70
- [115] Park H et al 2016 Enhanced energy transport in genetically engineered excitonic networks *Nat. Mater.* **15** 211–6
- [116] Plenio M B and Huelga S F 2008 Dephasing-assisted transport: quantum networks and biomolecules *New J. Phys.* **10** 113019
- [117] Chin A W, Datta A, Caruso F, Huelga S F and Plenio M B 2010 Noise-assisted energy transfer in quantum networks and light-harvesting complexes *New J. Phys.* **12** 065002
- [118] Hagelstein P L and Chaudhary I U 2015 Phonon models for anomalies in condensed matter nuclear science *Curr. Curr. Sci.* **108** 507–13 (available at: www.jstor.org/stable/24216595)
- [119] Hagelstein Peter L. 1998 Anomalous Energy Transfer In *Proc. Seventh Int. Conf. on Cold Fusion (19–24 April 1998, Vancouver, Canada)* pp 19–24
- [120] Ferry D K 1991 *Semiconductors* (Macmillan)
- [121] Pelc J S et al 2012 Downconversion quantum interface for a single quantum dot spin and 1550 nm single-photon channel *Opt. Express* **20** 27510–9
- [122] Wegh R T, Donker H, van Loef E V D, Oskam K D and Meijerink A 2000 Quantum cutting through downconversion in rare-earth compounds *J. Lumin* **87–89** 1017–9
- [123] Hagelstein P L 2023 Coherent nuclear dynamics for the nuclear part of LENR models *25th Int. Conf. on Condensed Matter Nuclear Science (Stettin, Poland, 27–31 August 2023)*
- [124] Möller P, Sierk A J, Bengtsson R, Sagawa H and Ichikawa T 2012 Nuclear shape isomers *At. Data Nucl. Data Tables* **98** 149–300
- [125] Sierk A J 1986 Macroscopic model of rotating nuclei *Phys. Rev. C* **33** 2039–53
- [126] Engel G S, Calhoun T R, Read E L, Ahn T-K, Mančal T, Cheng Y-C, Blankenship R E and Fleming G R 2007 Evidence for wavelike energy transfer through quantum coherence in photosynthetic systems *Nature* **446** 782–6
- [127] Lloyd S 2011 Quantum coherence in biological systems *J. Phys.: Conf. Ser.* **302** 012037
- [128] Hore P J 2015 *Nuclear Magnetic Resonance* (Oxford University Press)
- [129] Harris R K 1986 *Nuclear magnetic resonance spectroscopy* (Longman Scientific & Technical)
- [130] Bienfait A et al 2019 Phonon-mediated quantum state transfer and remote qubit entanglement *Science* **364** 368–71
- [131] Bocklage L, Gollwitzer J, Strohm C, Adolff C F, Schlage K, Sergeev I, Leupold O, Wille H-C, Meier G and Röhlberger R 2021 Coherent control of collective nuclear quantum states via transient magnons *Sci. Adv.* **7** eabc3991
- [132] Kōi Y, Tsujimura A, Hihara T and Kushida T 1961 Internal magnetic field in iron and iron alloys measured by NMR *J. Phys. Soc. Japan* **16** 1040
- [133] Berk C, Jaris M, Yang W, Dhuey S, Cabrini S and Schmidt H 2019 Strongly coupled magnon–phonon dynamics in a single nanomagnet *Nat. Commun.* **10** 1–6
- [134] Briggs J S and Eisfeld A 2011 Equivalence of quantum and classical coherence in electronic energy transfer *Phys. Rev. E* **83** 051911
- [135] Tycko R and Dabaghi G 1990 Measurement of nuclear magnetic dipole–dipole couplings in magic angle spinning NMR *Chem. Phys. Lett.* **173** 461–5
- [136] Hagelstein P 2016 Quantum composites: a review, and new results for models for condensed matter nuclear science *J. Condens. Matter Nucl. Sci.* **20** 139–225
- [137] Hagelstein P L 2018 Calculation of the boosted spin–orbit contribution to the phonon–nuclear coupling matrix element for ^{181}Ta *J. Condens. Matter Nucl. Sci.* **29** 392–400
- [138] Nassisi V 1998 Transmutation of elements in saturated palladium hydrides by an XeCl excimer laser *Fusion Technol.* **33** 468–75